frontiers | Frontiers in Materials

TYPE Original Research
PUBLISHED 23 September 2025
DOI 10.3389/fmats.2025.1643732

OPEN ACCESS

EDITED BY
Vincenzo Santinelli,
IRCCS San Donato Polyclinic, Italy

REVIEWED BY
Bhavani Patel,
Medline Industries, LP, United States
Sara E. Maloney Norcross,
RTI International, United States

*CORRESPONDENCE
Quan Ling,
Lynn18028389585@163.com

RECEIVED 11 June 2025
ACCEPTED 08 September 2025
PUBLISHED 23 September 2025

CITATION
Ling Q, Tian Y, Lv Z and Chen J (2025) Synthetic engineering of central venous catheter based on antibacterial endothelial simulation can effectively antagonize vascular infection and thrombosis.
Front. Mater. 12:1643732.
doi: 10.3389/fmats.2025.1643732

Synthetic engineering of central venous catheter based on antibacterial endothelial simulation can effectively antagonize vascular infection and thrombosis

Quan Ling*, Ye Tian, Zhu Lv and Jinling Chen

The First Department of Anesthesia, Zhongshan City People's Hospital, Zhongshan, China

Background: Infection remains a prevalent complication affecting long-term central venous catheter (CVC) implantation. While nitric oxide (NO) demonstrates dual antibacterial and immunomodulatory potential, the therapeutic application of BNN6—a near-infrared-responsive NO donor—in CVC materials requires systematic validation. This study developed a BNN6-integrated polyurethane-polydopamine (PU-PDA) composite coating for CVCs, assessing its structural stability, biosafety, antimicrobial efficacy, and immunoregulatory capacity.

Methods: The PU-PDA matrix was engineered to encapsulate BNN6 for controlled release of NO. Material characterization included hemocompatibility profiling (hemolysis/coagulation assays) and antibacterial validation against Gram-positive/negative strains. Immunomodulatory effects were evaluated through scratch wound healing, transwell migration, and inflammatory mediator expression assays, with intracellular NO dynamics quantified via fluorescence imaging.

Results: The composite coating exhibited optimal biocompatibility with negligible hemolytic activity (<2%). Bacterial proliferation was suppressed through NO-mediated metabolic disruption, while inflammatory cell motility demonstrated dose-dependent inhibition. Concurrently, upregulated intracellular NO correlated with reduced expression of pro-inflammatory cytokines (IL-6, TNF-α) and endothelial adhesion markers.

Conclusion: The BNN6-PU-PDA system achieves spatiotemporal NO delivery, effectively attenuating microbial colonization and host inflammatory cascades through modulation of inflammatory mediators. This dual-action mechanism positions the material as a promising strategy for infection-resistant CVC development.

KEYWORDS

central venous catheters, BNN6/PDA/PU composite, nitric oxide, immunomodulation, vascular infection

Introduction

The central venous catheter (CVC) is among the most widely utilized implantable medical devices in clinical applications. It is mainly applied in fields like rapid intravenous infusion, central venous pressure monitoring, blood collection, and continuous intravenous therapies such as chemotherapy. Long-term CVC implantation can give rise to a broad range of clinical complications, including thrombosis and infection (Citla Sridhar et al., 2020; Simonetti et al., 2020). The causes of thrombosis include three aspects: hypercoagulable state of the blood, hemodynamic changes, and activation of prothrombin. And the adhesion of leukocytes has been proven to be related to these three factors (Navarrete et al., 2023). Specifically, a hypercoagulable state can upregulate the expression of adhesion molecules on endothelial cells and leukocytes, promoting their interaction; abnormal hemodynamic changes reduce the shear force that resists leukocyte-endothelial contact, facilitating adhesion; and prothrombin activation generates thrombin, which directly stimulates leukocyte adhesion by activating protease-activated receptors (PARs) on their surface. Infection by pathogenic bacteria can also lead to the aggregation of leukocytes and the body's own immune response. Inhibiting the adhesion of leukocytes during the CVC insertion process is a feasible approach to reducing its clinical complications.

Nitric oxide (NO) is a diatomic molecular gas that can be produced by mammalian cells, and its synthesis is regulated by endogenous nitric oxide synthase (NOS) (Bredt, 1999). NO has been proven to be involved in various physiological processes such as cardiovascular function, metabolism, nerve excitability, and immune response (Andrabi et al., 2023; Lundberg and Weitzberg, 2022). Previous studies have shown that NO can inhibit the activation and aggregation of platelets and reduce the adhesion of inflammatory cells in blood vessels (Seabra et al., 2023; Matsushita et al., 2003). This suggests that we can utilize the properties related to NO to further control the adhesion of leukocytes in blood vessels (Ghalei et al., 2021). The antibacterial property of NO is dose-dependent. At low concentrations (usually below 1 μM), a limited bactericidal effect is shown by NO. Similar to eukaryotic cells, NO is an important biological signaling molecule in bacteria. Bacteria also have nitric oxide synthase (bacterial NOSs, bNOSs), but they lack the essential reductase domain. Therefore, the production of NO by bNOS requires the help of eukaryotic reductases *in vivo*. Studies have shown that bacteria can be protected from immune oxidative bursts, and the antibiotic resistance of bacteria can be increased by the NO produced by bNOS (Ghalei et al., 2021; Wang et al., 2022).

Materials for regulating NO release encapsulate special NO-releasable materials into specific carriers, and then control their release through a series of methods (Kim et al., 2022). While stimuli-responsive NO-releasing systems have been explored in fields like oncology (Li et al., 2022) (Shanmugam et al., 2014) (Kumari et al., 2020; Zhang et al., 2023) (Sun et al., 2021), their translation to CVCs remains limited. Previous work on NO-releasing catheters has primarily used non-responsive donors (e.g., S-nitrosothiols or N-diazeniumdiolates), leading to unregulated NO release that may compromise safety or efficacy (Brisbois et al., 2016a; Frost et al., 2005; Brisbois et al., 2016b; Pant et al., 2018; Ashcraft et al., 2022; Maloney et al., 2023). In contrast, photothermal triggering, with controllability, precision in time and space, and ease of operation, has attracted extensive attention. The photothermal effect after near-infrared (NIR) irradiation can trigger the release of NO in mesoporous polydopamine with a built-in plasmonic nanoparticle core (Yin et al., 2020; Wu et al., 2020).

BNN6 (N,N′-Di-sec-butyl-N,N′-dinitroso-1,4-phenylene diamine, a NIR-responsive NO donor) belongs to the category of Bis-N-nitroso compounds. These compounds are frequently utilized as NO donors and possess excellent thermal stability. The release of NO by these donors can be initiated by NIR, with a measurable release amount reaching up to 200 μM under 808 nm laser irradiation (1.5 W/cm^2) and sustained release over 72 h, while maintaining low biotoxicity. (Li et al., 2017; Huang et al., 2020). Biocompatible polydopamine nanoparticles (PDAs), structurally similar to naturally occurring melanin, were designed as both a PA imaging contrast agent and a chemo-thermotherapy therapy agent for tumors (Li et al., 2017). However, research on the application of nitric oxide donor BNN6 in CVC materials is limited. Therefore, materials with NIR-activated photothermal effects can be used to fabricate safe and reliable CVC. This material can reduce the adhesion of leukocytes and bacterial infections by controlling the release of nitric oxide (NO), thereby reducing the complications after CVC implantation. In this study, BNN6, polydopamine (PDA), and polyurethane (PU) were used to prepare a new type of CVC that responds to NIR and releases NO. Its antibacterial properties and biocompatibility were evaluated, so that the clinical application value could be assessed.

Methods

Materials and instruments

Fetal bovine serum (Excell Bio, China); dual-antibody (MACKLIN, China); DMEM medium, RPMI 1640 medium (Gibco, China); trypsin (Gibco, China); cell cryopreservation solution, PBS buffer (Beyotime, China); Tris-HCl (Biosharp, China); DA (Macklin, China); BNN6 (QIYUE, China); absolute ethanol (Guangzhou Brand Chemical Reagent, China); MTT Cell Proliferation and Cytotoxicity Assay Kit (Beyotime, China); Nitric Oxide Assay Kit (S0021S) (Beyotime, China); Cell Adhesion Assay Kit (V13181) (Thermo Fisher, United States); CRP ELISA Kit, IL-6 ELISA Kit, TNF-α ELISA Kit, FIB ELISA Kit, eNOS ELISA Kit, ICAM-1 ELISA Kit, VCAM-1 ELISA Kit (Hnybio, China); human umbilical vein cells EA.hy926, human monocyte THP-1 (both purchased from ATCC). Cell culture flasks T25, T75, 6-well plates, 96-well plates, 15 mL centrifuge tubes, 50 mL centrifuge tubes (Jet BIOFIL, China); enzyme-free pipette tips, 1.5 mL enzyme-free centrifuge tubes (KeyGEN, China); pipettors (Eppendorf); nitrile latex gloves (Loctite); CPE gloves (Guangming); central venous silicone catheters, central venous PU catheters (Cook Medical, China). Ultra-low-temperature freezer (Haier Company); optical microscope (Shanghai Optical Instrument Factory No.1); CO_2 cell culture incubator, super-clean workbench, constant-temperature water bath (Shanghai Boxun Industrial Medical Equipment Factory); liquid nitrogen tank YDS-175-276 (Huatie Gas Company); ultrapure water apparatus (ELGA Veoli Company); EVOS M5000 fluorescence microscope (Invitrogen by Thermo

Fisher, United States); RT-6000 microplate reader (Rayto Company); 2–16N high-speed normal-temperature centrifuge (Hunan Henuo Instrument and Equipment Co., Ltd.).

Sample preparation and experimental grouping

Polyurethane (PU) is one of the most commonly used materials for clinical CVCs, with well-documented biocompatibility and mechanical properties in patients (Console et al., 2007). PU was first cleaned with deionized water and then ultrasonically cleaned with absolute ethanol for 30 s before being dried and set aside. 0.10 g of PU material was taken and suspended in 1.00 mL of 1 mol/L Tris-HCl buffer solution with pH = 8.5. 0.03 g of DA was added at 30 °C and reacted for 20 h. Then, it was first cleaned with deionized water and then ultrasonically cleaned with absolute ethanol for 30 s before being dried to obtain a sample with a PDA coating on the surface (PDA/PU). The PDA/PU containing BNN6 was prepared by adding 1 mg/mL of BNN6 ethanol solution under the synthesis conditions of PDA/PU. The sample was cut into 1 mm × 1 mm in size and set aside.

The incubated slices were taken out, washed with water three times, and placed on a super-clean bench to be air-dried; crystal violet was added for staining for 1 min, and then the slices were washed with water. Iodine solution was added for staining for 1 min, and then the slices were washed with water. Decolorizing solution was added, shaken gently, the slices were decolorized for about 30 s, washed with water, air-dried, safranin was added, the slices were stained for 1 min, and then washed with water. The water was absorbed, and the slices were observed under a microscope and photographed.

Experimental analysis of crystal violet optical density

PU sheet and BNN6/PDA/PU sheet (size: 1 cm × 1 cm) samples were immersed in *Escherichia coli* or *Staphylococcus aureus* suspensions with a bacterial concentration of 2×10^7 CFU mL^{-1}, and were cultured for 14 days. Crystal violet staining was performed. After the samples were fully dissolved with a 33% acetic acid solution, the optical density value at 562 nm of the dissolved liquid was measured by a microplate reader.

Determination of hemolysis rate

10 mL of fresh rat blood was taken and centrifuged at 1500 rpm for 10 min. The supernatant was removed. The precipitated red blood cells were washed with PBS as described above until the supernatant showed no red color. A 2% suspension of the obtained red blood cells was prepared with PBS. Water was added as a positive control (PC), PBS was added as a negative control (NC), control (PU), and experiment (BNN6/PDA/PU). The mixture was incubated in a water bath at 37 °C for 1 h, centrifuged at 1000 rpm for 5 min, the supernatant was aspirated, and the OD600 absorption value was measured using an ultraviolet-visible spectrophotometer to calculate the hemolysis rate.

Hemolysis rate: Hemolysis rate (%) = (experimental group-negative control)/(positive control-negative control).

Thrombin time (TT) and plasma recalcification time (PRT)

The sheet was put into the plasma to be tested and incubated at 37 °C for 1 h. After incubation, the TT reagent, pre-warmed at 37 °C, was added, and the coagulation time TT value was recorded. The sheet was put into the plasma and soaked for 1 h, and PPP pre-incubated at 37 °C was added. Subsequently, according to the instructions of the kit, 0.025 mol/L $CaCl_2$ solution was added to each tube, and timing was started immediately. After 50 s, the centrifuge tube was tilted every 1–2 s to observe the coagulation state until it did not flow, and the coagulation time was recorded.

Immunofluorescence

1×10^4 macrophages were adhered to the surface of the PU sheet and the BNN6/PDA/PU sheet. At 0/1/3 days of culture, they were gently rinsed three times with PBS. 1 mL of 4% paraformaldehyde was added to fix the cells for 20 min. They were then gently rinsed three times with PBS. Triton - X100 was added for permeabilization for 20 min. After that, they were gently rinsed three times with PBS again. After serum blocking, 1 mL of CD34 primary antibody (1:200) was added and incubated overnight at 4 °C. Then, 1 mL of secondary antibody was added and incubated on a shaker at room temperature in the dark for 1 h. After being washed with TBST, they were stained with DAPI for 5 min. Pictures were taken under a fluorescence microscope, and the fluorescence intensity was analyzed using ImageJ software (National Institutes of Health, NIH).

CCK8 assay

2000 macrophages were adhered to the surface of the PU sheet and the BNN6/PDA/PU sheet. Six replicate wells were set up for each group. 10 μL of CCK8 solution was added to each well 2 h before the end of incubation at 0/1/3 days. After incubation, OD450 was measured with a microplate reader.

Cell culture

Culture of EA. hy926 cells: The cells were subcultured under the culture conditions of DMEM +10% FBS +1% P/S. When the cells fused to 80%, the old medium was discarded, and the cells were washed twice with 2 mL of PBS. After discarding PBS, 2 mL of 0.25% trypsin-0.02% EDTA mixed digestion solution was added. The cells were observed under a microscope. After about 30 s, when the cells became round, 6 mL of complete medium was quickly added to terminate digestion. The cells were gently blown and collected. They were centrifuged at 800 rpm, 4 °C for 5 min. The supernatant was discarded. The cells were resuspended with complete medium and cultured in separate flasks. The medium was changed every other day.

Culture of THP-1 cells: The cells were subcultured under the culture conditions of RPMI-1640 + 10% FBS +0.05 mM β-mercaptoethanol +1% P/S. 50% cell suspension was centrifuged (800–1000 rpm, 5 min), and 50% of the volume was replaced with fresh medium for culture.

Co-culture of CVC and EA.hy926 cells: CVCs made of silicone and PU materials were co-cultured with EA.hy926 cells, respectively. A 10 μL pipette tip was used to scratch the monolayer cells at the bottom of the well. After scratching, sterilized tweezers were used to pick up one cut CVC tube of 1 mm in size and gently put it into the cell culture medium of each well to culture with the cells (simulating the damage to vascular endothelial cells after CVC indwelling). Parallel groups without irradiation were included as controls. For irradiated groups, near-infrared light was irradiated through an 808 nm laser at a set intensity (1.0 W/cm^2) for a fixed time (5 min); preliminary tests evaluated the impact of different irradiation intensities (0.5–2.0 W/cm^2) on NO release to determine optimal parameters.

Wound healing assay

On the back of a 6-well plate, a tic-tac-toe pattern was drawn with parallel lines every 0.5 cm. After the cells in the logarithmic growth phase were digested and counted, 1×10^6 cells/well were inoculated into a 6-well plate. When the confluence of cells was more than 90%, the tip of a pipette tip was used to vertically abut against the lines marked on the back of the plate to make scratches. It was washed twice with PBS, and pictures were taken under a microscope to record the size of the cell scratch at 0 h. A cut CVC tube of 1 mm in size, made of different materials was picked up and gently put into the cell culture medium of each well. After culturing with the cells for 24 h, it was taken out and pictures were taken under a microscope to record the size of the cell scratch at 24 h.

Adhesion assay

EA.hy926 cells and THP-1 cells were processed. After being digested with trypsin and washed with PBS, they were collected in a centrifuge tube. They were centrifuged at 1000 rpm for 5 min and washed twice with PBS. They were resuspended to 1×10^6 cells/mL with the corresponding cell culture medium (without serum) to make a cell suspension (THP-1 did not need digestion) and then inoculated into a 6-well plate. A cell damage model was constructed according to the grouping; 10 μL of calcein AM (component A) was added to the 6-well plate to reach a final concentration of 5 μM. They were incubated at 37 °C for 30 min; the cells were washed twice with DMEM or 1640 culture medium preheated at 37 °C; the cell fluorescence intensity was detected and pictures were taken with a fluorescence microscope.

Detection of NO level

Intracellular NO levels were detected using a nitric oxide assay kit, which measures nitrite (a stable metabolite of NO) as a proxy for NO levels. Cells were lysed and centrifuged, and the supernatant was collected. The reaction mixture was prepared according to the kit instructions, and absorbance was measured at 540 nm using a microplate reader. Briefly, Griess Reagent I and II were taken out and allowed to return to room temperature. The 1M standard substance was diluted with the corresponding cell culture medium to 10, 20, 40, 60, 80, and 100 μM, respectively. The standard substance and supernatant of cell culture medium were added at 50 μL/well in a 96-well plate. After 50 μL of Griess Reagent I and Griess Reagent II were added to each well, the absorbance at 540 nm was measured. A standard curve was drawn, and the corresponding concentration of the sample was calculated.

ELISA

The supernatant of each group of cells treated according to the grouping was taken. It was centrifuged at 200 *g* for 5 min. The supernatant after centrifugation was taken as the sample. The standard substance was diluted with the standard substance dilution solution according to the respective instructions. 50 μL of the standard substance was added to the enzyme-labeled coated plate. 25 μL of sample dilution solution was added to the wells for test samples first, and then 25 μL of test sample was added. The plate was sealed with a sealing film and incubated at 37 °C for 30 min. The washing solution was filled into each well. It was left standing for 30 s and then discarded. This was repeated 5 times. 50 μL of enzyme-labeled reagent was added and incubated at 37 °C for 30 min. Then it was washed again. 100 μL of chromogenic reagent was added to each well first. Color was developed at 37 °C in the dark for 15 min. Then, 50 μL of termination solution was added to each well to terminate the reaction. The absorbance at 450 nm of each well was measured.

Data analysis

Data was analyzed and graphed using GraphPad Prism 9 (Version 9.5.0). The graphs were organized and combined using Adobe Illustrator. All plots were expressed as means ± SD. The statistical differences between groups were tested by the T-Test. A P value less than 0.05 was considered a significant difference. (*indicated $P < 0.05$, **indicated $P < 0.01$, and ***indicated $P < 0.001$).

Result

BNN6/PDA/PU material could stably release NO

The biological safety of implantable materials is a very important indicator. We tested whether this material would cause coagulation or hemolysis events. This material was placed in a freshly prepared rat erythrocyte suspension, and its hemolysis rate was detected. It was found that compared with the PU group, a stronger anti-hemolytic effect was had by the BNN6/PDA/PU material (Figure 1B). At the same time, the two materials were

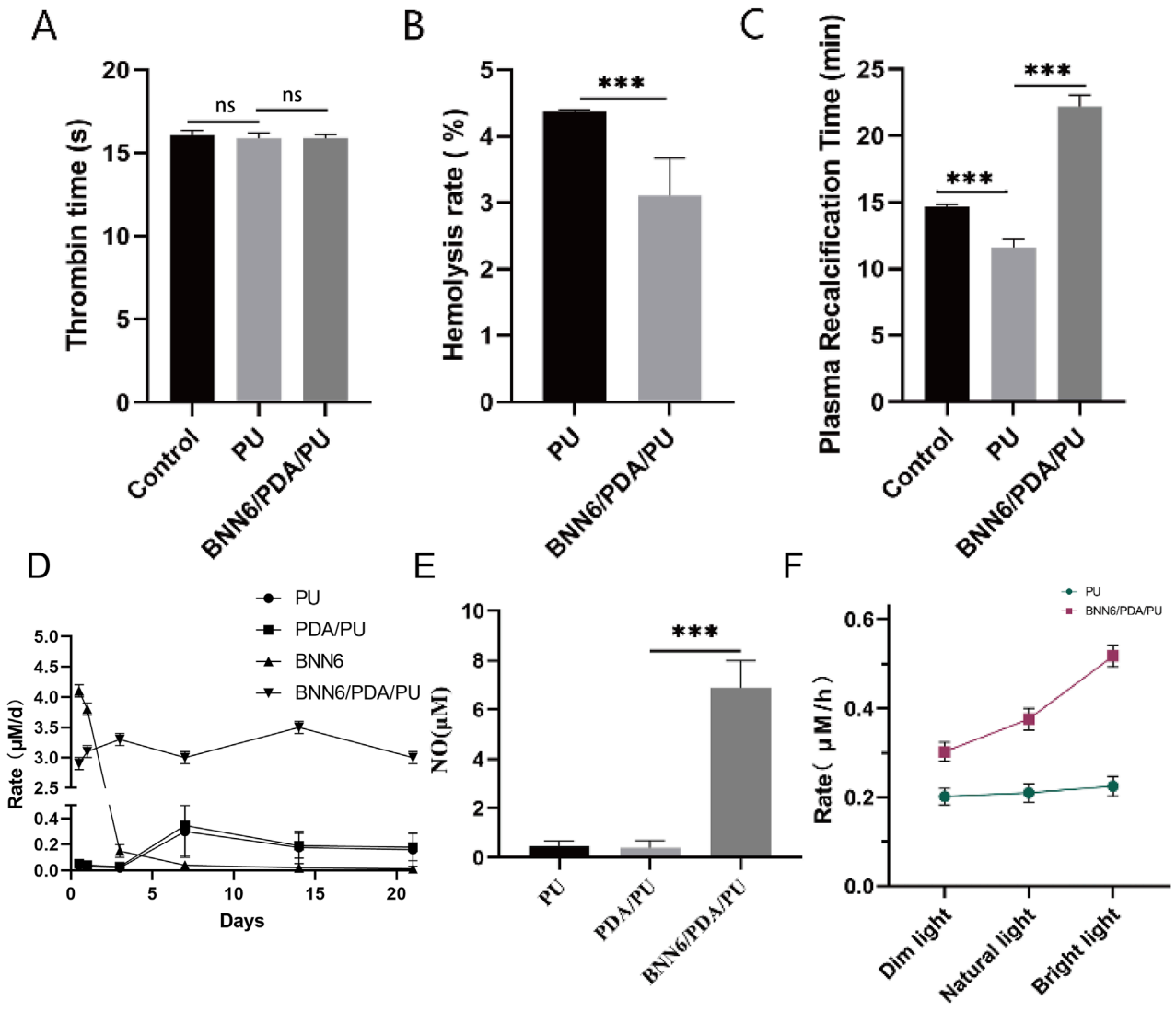

FIGURE 1
BNN6/PDA/PU material could stably release NO. **(A)** Thrombin time under different materials. **(B)** Hemolysis rate under different materials. **(C)** Plasma recalcification time under different materials. **(D)** Rate of NO generation over time. **(E)** Intracellular NO concentration changes caused by BNN6/PDA/PU. **(F)** Rate of NO generation with increasing near-infrared illumination intensity. $^{**}p < 0.01$, $^{***}p < 0.001$.

placed in rat plasma, and their thrombin time and plasma recalcification time were detected. It was found that no difference in thrombin time was found compared with the control group or the PU group (Figure 1A), while the plasma recalcification time was significantly increased (Figure 1C). It was suggested by these indicators that no effect on blood status is had by the BNN6/PDA/PU material.

The changes in its performance after being soaked in PBS for different times were also detected to verify the stability of this material. The BNN6 group exhibited a rapid initial NO release rate but showed negligible NO release after day 1, indicating the intrinsic NO-releasing capacity of BNN6 but its lack of sustained release. In contrast, the BNN6/PDA/PU group maintained stable NO release for up to 21 days, with a sustained release rate, demonstrating that the PDA/PU matrix effectively prolonged the NO release profile of BNN6. The PU and PDA/PU groups showed minimal NO release, confirming that BNN6 is the primary source of NO generation in the composite coating (Figure 1D). After this material was co-cultured with cells cultured *in vitro*, it could also be detected that a significant increase in intracellular NO concentration had been caused by the BNN6/PDA/PU material (Figure 1E). This elevation was specific to the BNN6-containing group, as PU and PDA/PU controls showed no comparable increase, confirming that BNN6 is the critical factor driving NO elevation. Performance and stability tests were conducted on the newly synthesized material. It was observed that under near-infrared illumination conditions, preliminary tests evaluated multiple intensities (0.5–2.0 W/cm^2) and confirmed that as the illumination intensity increases, the rate of NO generation by the BNN6/PDA/PU material also increases (Figure 1F). Consistent results were obtained in both irradiated (1.0 W/cm^2, 5 min) and non-irradiated groups, with non-irradiated controls showing minimal NO release.

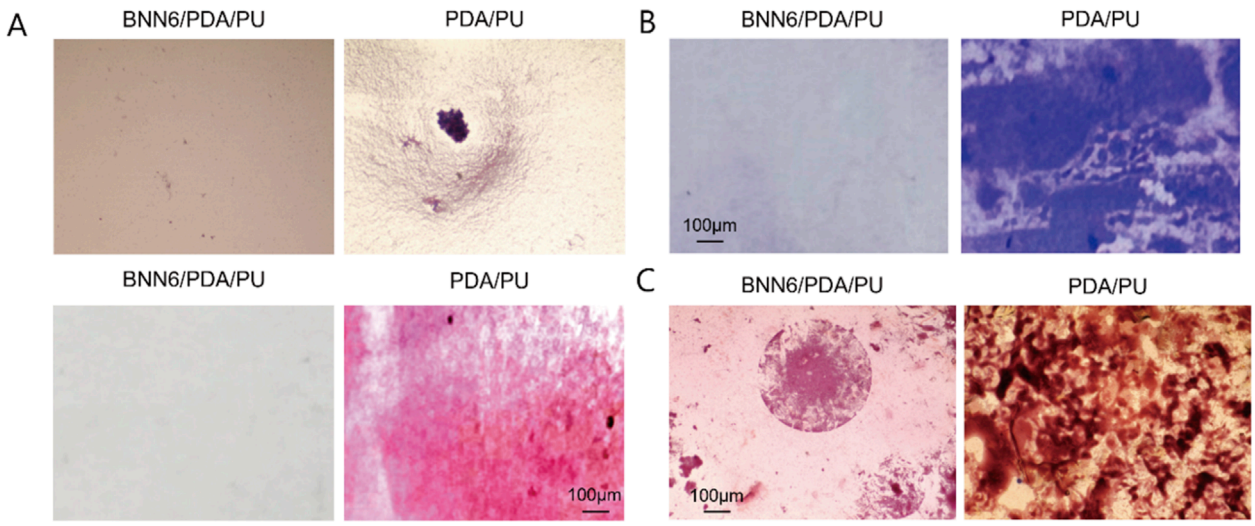

FIGURE 2
BNN6/PDA/PU material could effectively inhibit the growth of bacteria. **(A)** Light microscope and Gram staining results under bacterial growth in different materials. **(B)** Crystal violet density staining. **(C)** Gram staining results of bacterial growth in different groups after incubation for 14 days.

BNN6/PDA/PU material could effectively inhibit the growth of bacteria

As an implantable CVC material, we focused on evaluating its antibacterial performance. First, *Staphylococcus aureus* was cultured on BNN6/PDA/PU material and PU material to observe the inhibitory ability of BNN6/PDA/PU material on bacteria. It could be seen that the bacteria count on BNN6/PDA/PU material was significantly lower than that on PU material (Figure 2A). Since bacteria adhered under natural conditions and formed a biofilm to resist the action of drugs, which was very common in implantable materials. Therefore, crystal violet density experiments were used to observe the ability of bacteria to form biofilms. It was found that the area of bacterial biofilm on BNN6/PDA/PU material was significantly lower than that on PU material, suggesting that the ability of bacteria to form biofilms was inhibited (Figure 2B). At the same time, whether the antibacterial performance of the BNN6/PDA/PU material was stable was investigated. After the two materials were incubated in a suspension of *Staphylococcus aureus* for 14 days, the number of bacteria was observed again. It was found that the number of bacteria in BNN6/PDA/PU material was still lower than that in PU material after 14 days (Figure 2C). This suggested that antibacterial properties were still maintained within 14 days. The goal here was to reduce bacterial adhesion, as it is a precursor to biofilm formation and infection.

BNN6/PDA/PU material could significantly inhibit the growth of leukocytes

Sheets of different materials were co-cultured with the leukocyte line, and the wound healing assay was used to detect the impact of these materials on the cell state to detect the biological safety of the BNN6/PDA/PU material. It was found that among various sheets, the BNN6/PDA/PU material was most similar to the control group in state, and the migration of leukocytes could be significantly inhibited by it, while the migration of leukocytes would be promoted by the stimulation of other materials (Figures 3A,B). The goal of this assay was to evaluate whether the coating could reduce excessive leukocyte migration to the CVC insertion site, as uncontrolled leukocyte infiltration can lead to prolonged inflammation and tissue damage.

The wound healing assay cannot completely determine whether the adhesion ability of leukocytes has decreased. Therefore, a cell adhesion assay was used to evaluate the adhesion of leukocytes. Leukocytes were incubated with different sheets, and immunofluorescence was used to analyze the number of cells in each group so that the adhesion-related ability of leukocytes could be detected. Among them, the adhesion ability of EA.hy926 and THP-1 cells in the PU group was significantly lower than that in the silicone group and the blank group; while the adhesion ability of EA.hy926 and THP-1 cells in the BNN6/PDA/PU group was significantly lower than that in the PDA/PU group and the blank group (Figures 4A–C). It is suggested that a good anti-inflammatory cell adsorption effect is had by the BNN6/PDA/PU sheet.

Subsequently, macrophage adhesion experiments were conducted by using PU sheets and BNN6/PDA/PU sheets, and the number of $CD34^+$ cells was detected after 3 days. It was found that fewer macrophages were present in the BNN6/PDA/PU sheets (Figures 4D,E). At the same time, the activity of the two groups of cells was detected at 0/1/3 days, respectively. It was found that although the activity of macrophages increased with time, good performance in inhibiting macrophage activity was still shown by the BNN6/PDA/PU sheets compared to PU sheets (Figure 4F).

Expression of related molecules

To better understand the performance of BNN6/PDA/PU material, the inflammatory factors and NO synthesis-related

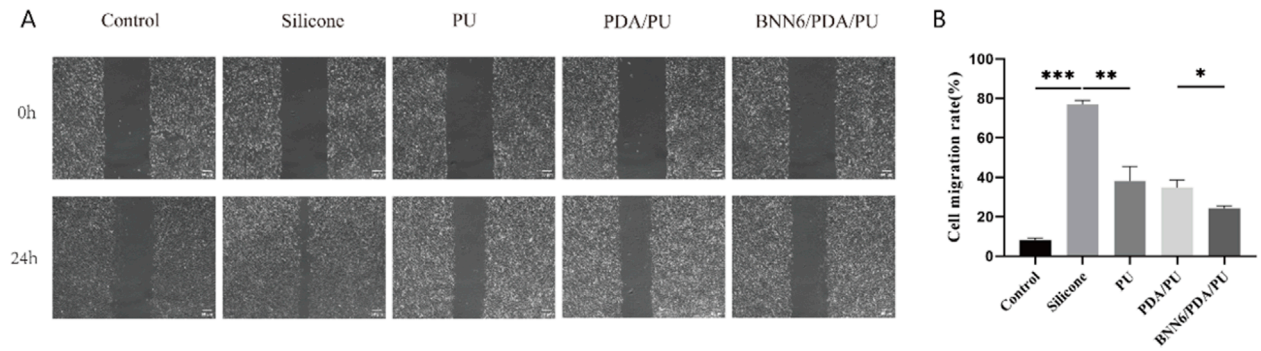

FIGURE 3
Wound healing assay. **(A)** Leukocyte wound healing assay under different groups, with the silicone group as a positive control. **(B)** Statistical chart of cell wound healing assays in different groups, n = 6. $^{*}p < 0.05$, $^{**}p < 0.01$, $^{***}p < 0.001$.

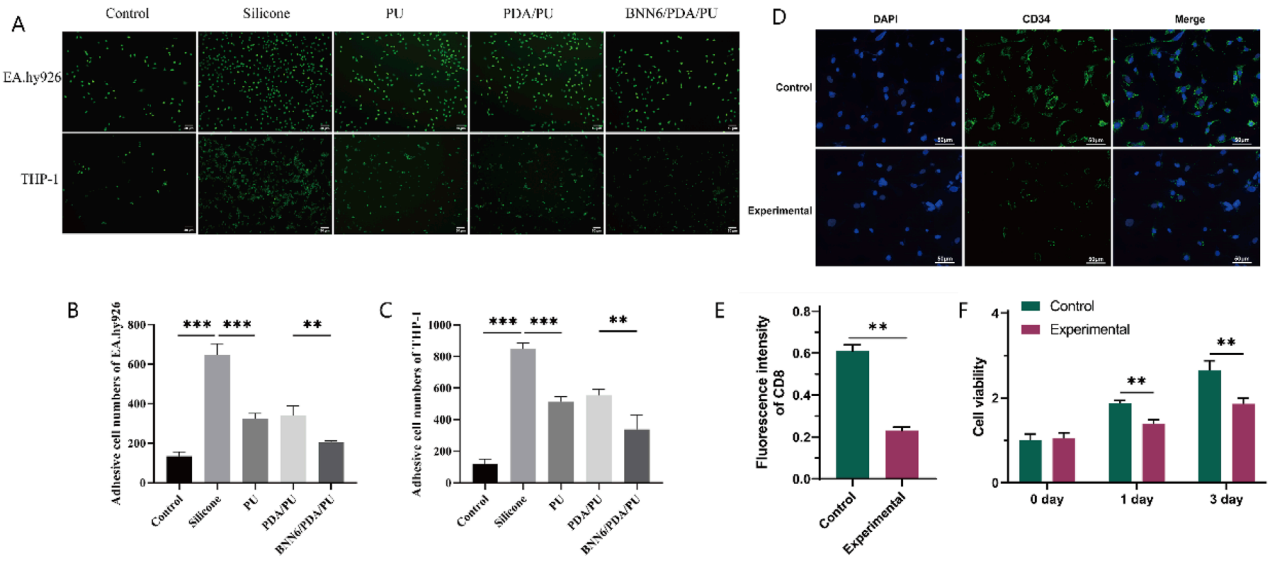

FIGURE 4
Adhesion Assay. **(A)** Immunofluorescence results of the adhesion of human umbilical vein cells and monocytes. **(B)** Quantitative analysis graph of immunofluorescence results of human umbilical vein cells, n = 6. **(C)** Quantitative analysis graph of immunofluorescence results of monocytes, n = 6. **(D)** Immunofluorescence results of the long-term adsorption experiment of macrophages. **(E)** Quantitative analysis graph of immunofluorescence results of the long-term adsorption experiment of macrophages, n = 6. **(F)** Graph of changes in macrophage activity detected by CCK-8 over time, n = 6. $^{*}p < 0.05$, $^{**}p < 0.01$, $^{***}p < 0.001$.

proteins of different materials were analyzed. The expression levels of CRP, IL-6, TNF-α, FIB, eNOS, ICAM-1, and VCAM-1 factors in EA.hy926 cells in the BNN6/PDA/PU group were statistically different from those in the PDA/PU group (Figure 5). Moreover, compared with the BNN6 group, the BNN6/PDA/PU group exhibited more potent suppression of key inflammatory cytokines (CRP, IL-6, TNF-α) and adhesion molecules (ICAM-1, VCAM-1). It was suggested that the expression of inflammatory factors could be significantly reduced by the BNN6/PDA/PU material based on the PU material. This inhibitory effect on inflammatory factors was related to the synthesis of NO. The decreased expression of coagulation factors and intercellular adhesion factors also indicated that the risk of thrombosis was effectively inhibited.

Discussion

In this study, a PDA and PU reaction system was used to construct a CVC with a PDA coating, and the light-sensitive material BNN6 was embedded in the PDA layer to endow it with the ability to control NO release, and the adhesion ability of EA.hy926 cells and THP-1 cells was evaluated. Previous studies have confirmed that BNN6 can release NO under NIR stimulation and has been applied in anti-bacterial infection (Zhou et al., 2022). We first conducted a cell adhesion experiment and not only found that cell adhesion in the BNN6/PDA/PU group was inhibited, but also proved that this material had no significant effect on cell activity, suggesting that this material is safe and reliable. At the same time, compared with traditional PU materials, BNN6/PDA/PU

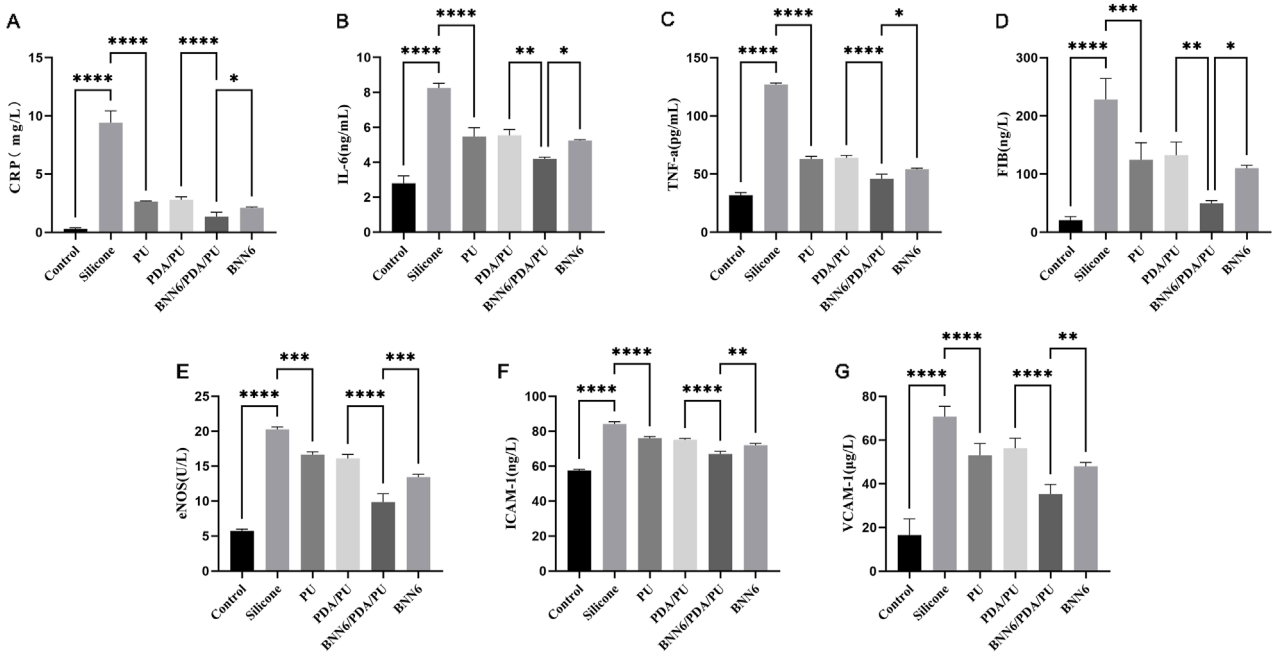

FIGURE 5
ELISA experimental results of inflammatory molecules, adhesion-related molecules and NO metabolism-related molecules. **(A)** Expression of C-reactive protein in different materials, n = 6. **(B)** Expression of inflammatory factor interleukin-6 under stimulation of different materials, n = 6. **(C)** Expression of inflammatory factor tumor necrosis factor-α under stimulation of different materials, n = 6. **(D)** Expression of fibrinogen under stimulation of different materials, n = 6. **(E)** Expression of endothelial nitric oxide synthase under stimulation of different materials, n = 6. **(F)** Expression of cell adhesion molecule-1 under stimulation of different materials, n = 6. **(G)** Expression of vascular cell adhesion molecule-1 under stimulation of different materials, n = 6. $^{*}p < 0.05$, $^{**}p < 0.01$, $^{***}p < 0.001$.

shows more excellent characteristics in inhibiting cell migration and adhesion. Finally, we have determined that NO inhibits the adhesion of leukocytes by reducing the expression of multiple inflammatory factors.

Although there are standardized operations by professional physicians, the complication rate after CVC placement is still as high as 3% (Teja et al., 2024). This is caused by changes in hemodynamics and blood components caused by long-term placement and chronic immune rejection. As a widely existing cell type in the blood, the aggregation of leukocytes near the CVC or blood vessel wall will cause inflammatory cell infiltration and hypercoagulability of the blood, thereby promoting vascular inflammation and thrombosis formation. In severe cases, even adhesion between the catheter wall and blood vessels will occur, causing difficulty in extubation. At present, the conventional way to avoid thrombosis after CVC placement is to take anticoagulant drugs. The perspective of using appropriate materials to avoid such complications has received less attention. Inhibiting cell adhesion on CVC through appropriate biocompatible materials can fundamentally eliminate such problems (Wu et al., 2023).

Previous studies have also found that NO-releasing catheters (e.g., hemodialysis and central venous catheters) can effectively inhibit the adhesion of bacteria and proteins, demonstrating significant anti-infection and anti-thrombotic effects (Maloney et al., 2023; Pant et al., 2017; Brisbois et al., 2013; Frost and Meyerhoff, 2004). While we found that BNN6/PDA/PU has the effect of inhibiting cell adhesion, we detected the concentration of NO and found that the intracellular NO concentration was significantly increased. Such results are consistent with previous reports. Considering that different concentrations of NO have two-sided effects on the regulation of cell physiological functions. For example, high concentrations of NO will inhibit the growth of tumor cells, while low concentrations of NO show a tumor-promoting effect (Dios-B et al., 2022). We believe that the concentration of NO released by BNN6/PDA/PU can reach the working concentration that has a negative regulatory effect on cell adhesion and the like.

To establish an exact connection between NO level and cell adhesion, we detected the expression of cell-related adhesion molecules and found that the expression of adhesion molecules in the BNN6/PDA/PU group was significantly lower than that in other treatment groups, suggesting that NO at this concentration can inhibit the expression of adhesion molecules (Pearl et al., 2012). At the same time, the expression of inflammatory factors, including TNF-α and IL-6, was also inhibited, suggesting that NO can prevent inflammatory reactions (Scumpia et al., 2004) after CVC placement. It is worth noting that exogenous NO release will cause an increase in intracellular NO concentration and a decrease in nitric oxide synthase activity, which may be the effect of negative feedback regulation (Chen et al., 2001). These results indicate that the BNN6/PDA/PU material can release NO through NIR response, increase the intracellular NO level, and then inhibit the expression of cell adhesion molecules, thereby inhibiting cell adhesion and migration and reducing the

inflammatory response of cells. Our results also demonstrate that BNN6 is the core NO-releasing component in the composite coating, as evidenced by the rapid initial NO release in the BNN6 alone group. However, the short duration of NO release from BNN6 alone limits its long-term biological efficacy. In contrast, the BNN6/PDA/PU coating maintains stable NO release for 21 days, and this sustained release translates to enhanced biological effects. This sustained NO release is essential for long-term medical devices like CVCs, where prolonged inhibition of inflammation and cell adhesion is required to prevent complications such as thrombosis and infection. The synergistic effect between BNN6 and the PDA/PU matrix not only leverages BNN6's NO-releasing property but also overcomes its inherent limitation of rapid exhaustion, thereby optimizing the biological performance of the coating.

Our research also has certain limitations. For example, we did not use scanning electron microscopy to analyze the surface coating of the new material. Notably, as a surface coating dependent on pre-loaded NO donors (BNN6), the system has an inherent limitation: once the NO supply is exhausted, additional NO cannot be regenerated, which may restrict long-term efficacy. This is mainly because our research focus is on its clinical application. With respect to the clinical translation of the BNN6-PDA-PU coating, the expected use time of the coating is designed to match the typical clinical service cycle of central venous catheters (CVCs), which usually ranges from several weeks to several months; accordingly, the NO release duration of the coating is expected to last at least throughout the standard CVC usage period to maintain sustained anti-thrombotic and anti-infective effects. For the irradiation process, intermittent NIR irradiation (e.g., short-duration irradiation once daily) is tentatively considered, as it is more clinically feasible than continuous irradiation and aligns with routine patient care schedules. Optimal parameters for the coating's use time, NO release duration, and irradiation protocol will be systematically evaluated in future animal and clinical studies. We will consider improving the structural analysis of the new material in subsequent work. Additionally, while we included non-irradiated controls and evaluated irradiation intensity effects, dedicated experiments to isolate the independent impact of light were not performed. This will be addressed in future studies to further clarify light-induced cellular responses. In subsequent studies, we will focus on the performance of such materials in animal experiments and explore their biosafety performance. At the same time, considering the good NIR response characteristics of this material and the performance of controlling NO release, it can be used as a controllable material for fine control of external NO exposure in subsequent studies.

Conclusion

In conclusion, our research constructed a new type of CVC material that could release NO in response to near-infrared irradiation. It was demonstrated that this material had good stability and biocompatibility while effectively inhibiting the adhesion of leukocytes and the growth of bacteria. This suggested its potential value as a new type of CVC material for clinical application.

Data availability statement

The original contributions presented in the study are included in the article/supplementary material, further inquiries can be directed to the corresponding author.

Author contributions

QL: Conceptualization, Project administration, Writing – review and editing, Data curation, Validation, Methodology, Writing – original draft, Funding acquisition, Formal Analysis, Visualization. YT: Writing – review and editing, Data curation, Supervision, Writing – original draft, Conceptualization, Resources. ZL: Validation, Supervision, Data curation, Writing – review and editing. JC: Formal Analysis, Conceptualization, Validation, Writing – review and editing.

Funding

The author(s) declare that financial support was received for the research and/or publication of this article. This study was supported by the Guangdong Province Medical Science and Technology Research Fund Project (A2022336) and Zhongshan City Social Welfare Science and Technology Research Project (2022B1101).

Acknowledgments

The authors are grateful to all participants in the present study.

Conflict of interest

The authors declare that the research was conducted in the absence of any commercial or financial relationships that could be construed as a potential conflict of interest.

Generative AI statement

The author(s) declare that no Generative AI was used in the creation of this manuscript.

Any alternative text (alt text) provided alongside figures in this article has been generated by Frontiers with the support of artificial intelligence and reasonable efforts have been made to ensure accuracy, including review by the authors wherever possible. If you identify any issues, please contact us.

Publisher's note

References

Andrabi, S. M., Sharma, N. S., Karan, A., Shahriar, S. M. S., Cordon, B., Ma, B., et al. (2023). Nitric oxide: physiological functions, delivery, and biomedical applications. *Adv. Sci. (Weinh)* 10 (30), e2303259. doi:10.1002/advs.202303259

Ashcraft, M., Douglass, M., Garren, M., Mondal, A., Bright, L. E., Wu, Y., et al. (2022). Nitric oxide-releasing lock solution for the prevention of catheter-related infection and thrombosis. *ACS Appl. Bio Mater* 5 (4), 1519–1527. doi:10.1021/acsabm.1c01272

Bredt, D. S. (1999). Endogenous nitric oxide synthesis: biological functions and pathophysiology. *Free Radic. Res.* 31 (6), 577–596. doi:10.1080/10715769900301161

Brisbois, E. J., Handa, H., Major, T. C., Bartlett, R. H., and Meyerhoff, M. E. (2013). Long-term nitric oxide release and elevated temperature stability with S-nitroso-N-acetylpenicillamine (SNAP)-Doped Elast-eon E2As polymer. *Biomaterials* 34 (28), 6957–6966. doi:10.1016/j.biomaterials.2013.05.063

Brisbois, E. J., Kim, M., Wang, X., Mohammed, A., Major, T. C., Wu, J., et al. (2016a). Improved hemocompatibility of multilumen catheters via nitric oxide (NO) release from S-Nitroso-N-acetylpenicillamine (SNAP) composite filled lumen. *ACS Appl. Mater Interfaces* 8 (43), 29270–29279. doi:10.1021/acsami.6b08707

Brisbois, E. J., Major, T. C., Goudie, M. J., Meyerhoff, M. E., Bartlett, R. H., and Handa, H. (2016b). Attenuation of thrombosis and bacterial infection using dual function nitric oxide releasing central venous catheters in a 9day rabbit model. *Acta Biomater.* 44, 304–312. doi:10.1016/j.actbio.2016.08.009

Chen, J. X., Berry, L. C., Tanner, M., Chang, M., Myers, R. P., and Meyrick, B. (2001). Nitric oxide donors regulate nitric oxide synthase in bovine pulmonary artery endothelium. *J. Cell Physiol.* 186 (1), 116–123. doi:10.1002/1097-4652(200101)186:1<116::aid-jcp1005>3.0.co;2-x

Citla Sridhar, D., Abou-Ismail, M. Y., and Ahuja, S. P. (2020). Central venous catheter-related thrombosis in children and adults. *Thromb. Res.* 187, 103–112. doi:10.1016/j.thromres.2020.01.017

Console, G., Calabrò, C., Nardulli, P., Digiuseppe, F., Rucci, A., Russo, P., et al. (2007). Clinical and economic effects of central venous catheters on oncology patient care. *J. Chemother.* 19 (3), 309–314. doi:10.1179/joc.2007.19.3.309

Dios-Barbeito, S., González, R., Cadenas, M., García, L. F., Victor, V. M., Padillo, F. J., et al. (2022). Impact of nitric oxide in liver cancer microenvironment. *Nitric Oxide* 128, 1–11. doi:10.1016/j.niox.2022.07.006

Frost, M. C., and Meyerhoff, M. E. (2004). Controlled photoinitiated release of nitric oxide from polymer films containing S-nitroso-N-acetyl-DL-penicillamine derivatized fumed silica filler. *J. Am. Chem. Soc.* 126 (5), 1348–1349. doi:10.1021/ja039466i

Frost, M. C., Reynolds, M. M., and Meyerhoff, M. E. (2005). Polymers incorporating nitric oxide releasing/generating substances for improved biocompatibility of blood-contacting medical devices. *Biomaterials* 26 (14), 1685–1693. doi:10.1016/j.biomaterials.2004.06.006

Ghalei, S., Li, J., Douglass, M., Garren, M., and Handa, H. (2021). Synergistic approach to develop antibacterial electrospun scaffolds using honey and S-Nitroso-N-acetyl penicillamine. *ACS Biomater. Sci. Eng.* 7 (2), 517–526. doi:10.1021/acsbiomaterials.0c01411

Huang, S., Liu, H., Liao, K., Hu, Q., Guo, R., and Deng, K. (2020). Functionalized GO nanovehicles with nitric oxide release and photothermal activity-based hydrogels for bacteria-infected wound healing. *ACS Appl. Mater Interfaces* 12 (26), 28952–28964. doi:10.1021/acsami.0c04080

Kim, T., Nah, Y., Kim, J., Lee, S., and Kim, W. J. (2022). Nitric-oxide-modulatory materials for biomedical applications. *Acc. Chem. Res.* 55 (17), 2384–2396. doi:10.1021/acs.accounts.2c00159

Kumari, R., Sunil, D., and Ningthoujam, R. S. (2020). Hypoxia-responsive nanoparticle based drug delivery systems in cancer therapy: an up-to-date review. *J. Control Release* 319, 135–156. doi:10.1016/j.jconrel.2019.12.041

Li, Y., Jiang, C., Zhang, D., Wang, Y., Ren, X., Ai, K., et al. (2017). Targeted polydopamine nanoparticles enable photoacoustic imaging guided chemo-photothermal synergistic therapy of tumor. *Acta Biomater.* 47, 124–134. doi:10.1016/j.actbio.2016.10.010

Li, Y., Yoon, B., Dey, A., Nguyen, V. Q., and Park, J. H. (2022). Recent progress in nitric oxide-generating nanomedicine for cancer therapy. *J. Control Release* 352, 179–198. doi:10.1016/j.jconrel.2022.10.012

Lundberg, J. O., and Weitzberg, E. (2022). Nitric oxide signaling in health and disease. *Cell* 185 (16), 2853–2878. doi:10.1016/j.cell.2022.06.010

Maloney, S. E., Grayton, Q. E., Wai, C., Uriyanghai, U., Sidhu, J., Roy-Chaudhury, P., et al. (2023). Nitric oxide-releasing hemodialysis catheter lock solutions. *ACS Appl. Mater Interfaces* 15 (24), 28907–28921. doi:10.1021/acsami.3c02506

Matsushita, K., Morrell, C. N., Cambien, B., Yang, S. X., Yamakuchi, M., Bao, C., et al. (2003). Nitric oxide regulates exocytosis by S-nitrosylation of N-ethylmaleimide-sensitive factor. *Cell* 115 (2), 139–150. doi:10.1016/s0092-8674(03)00803-1

Navarrete, S., Solar, C., Tapia, R., Pereira, J., Fuentes, E., and Palomo, I. (2023). Pathophysiology of deep vein thrombosis. *Clin. Exp. Med.* 23 (3), 645–654. doi:10.1007/s10238-022-00829-w

Pant, J., Goudie, M. J., Hopkins, S. P., Brisbois, E. J., and Handa, H. (2017). Tunable nitric oxide release from S-Nitroso-N-acetylpenicillamine via catalytic copper nanoparticles for biomedical applications. *ACS Appl. Mater Interfaces* 9 (18), 15254–15264. doi:10.1021/acsami.7b01408

Pant, J., Goudie, M. J., Chaji, S. M., Johnson, B. W., and Handa, H. (2018). Nitric oxide releasing vascular catheters for eradicating bacterial infection. *J. Biomed. Mater Res. B Appl. Biomater.* 106 (8), 2849–2857. doi:10.1002/jbm.b.34065

Pearl, J. E., Torrado, E., Tighe, M., Fountain, J. J., Solache, A., Strutt, T., et al. (2012). Nitric oxide inhibits the accumulation of CD4+CD44hiTbet+CD69lo T cells in mycobacterial infection. *Eur. J. Immunol.* 42 (12), 3267–3279. doi:10.1002/eji.201142158

Scumpia, P. O., Sarcia, P. J., Kelly, K. M., DeMarco, V. G., and Skimming, J. W. (2004). Hypothermia induces anti-inflammatory cytokines and inhibits nitric oxide and myeloperoxidase-mediated damage in the hearts of endotoxemic rats. *Chest* 125 (4), 1483–1491. doi:10.1378/chest.125.4.1483

Seabra, A. B., Pieretti, J. C., de Melo Santana, B., Horue, M., Tortella, G. R., and Castro, G. R. (2023). Pharmacological applications of nitric oxide-releasing biomaterials in human skin. *Int. J. Pharm.* 630, 122465. doi:10.1016/j.ijpharm.2022.122465

Shanmugam, V., Selvakumar, S., and Yeh, C. S. (2014). Near-infrared light-responsive nanomaterials in cancer therapeutics. *Chem. Soc. Rev.* 43 (17), 6254–6287. doi:10.1039/c4cs00011k

Simonetti, G., Sommariva, A., Lusignani, M., Anghileri, E., Ricci, C. B., Eoli, M., et al. (2020). Prospective observational study on the complications and tolerability of a peripherally inserted central catheter (PICC) in neuro-oncological patients. *Support. Care Cancer* 28 (6), 2789–2795. doi:10.1007/s00520-019-05128-x

Sun, X., Li, L., Zhang, H., Dong, M., Wang, J., Jia, P., et al. (2021). Near-infrared light-regulated drug-food homologous bioactive molecules and photothermal collaborative precise antibacterial therapy nanoplatform with controlled release property. *Adv. Healthc. Mater.* 10 (16), 2100546. doi:10.1002/adhm.202100546

Teja, B., Bosch, N. A., Diep, C., Pereira, T. V., Mauricio, P., Sklar, M. C., et al. (2024). Complication rates of central venous catheters: a systematic review and meta-analysis. *JAMA Intern Med.* 184 (5), 474–482. doi:10.1001/jamainternmed.2023.8232

Wang, J., Rao, L., Huang, Z., Ma, L., Yang, T., Yu, Z., et al. (2022). The nitric oxide synthase gene negatively regulates biofilm formation in Staphylococcus epidermidis. *Front. Cell Infect. Microbiol.* 12, 1015859. doi:10.3389/fcimb.2022.1015859

Wu, D., Zhou, J., Chen, X., Chen, Y., Hou, S., Qian, H., et al. (2020). Mesoporous polydopamine with built-in plasmonic core: traceable and NIR triggered delivery of functional proteins. *Biomaterials* 238, 119847. doi:10.1016/j.biomaterials.2020.119847

Wu, M., Liu, H., Zhu, Y., Chen, F., Chen, Z., Guo, L., et al. (2023). Mild photothermal-stimulation based on injectable and photocurable hydrogels orchestrates immunomodulation and osteogenesis for high-performance bone regeneration. *Small* 19 (28), e2300111. doi:10.1002/smll.202300111

Yin, H., Guan, X., Lin, H., Pu, Y., Fang, Y., Yue, W., et al. (2020). Nanomedicine-enabled photonic thermogaseous cancer therapy. *Adv. Sci. (Weinh)* 7 (2), 1901954. doi:10.1002/advs.201901954

Zhang, S., Li, M., Wang, J., Zhou, Y., Dai, P., Zhao, M., et al. (2023). NIR-triggered On-Demand nitric oxide release for enhanced synergistic phototherapy of hypoxic tumor. *Bioconjug Chem.* 34 (7), 1327–1335. doi:10.1021/acs.bioconjchem.3c00250

Zhou, Y., Wu, W., Yang, P., Mao, D., and Liu, B. (2022). Near-infrared chemiluminescent nanoprobes for deep imaging and synergistic photothermal-nitric-oxide therapy of bacterial infection. *Biomaterials* 288, 121693. doi:10.1016/j.biomaterials.2022.121693